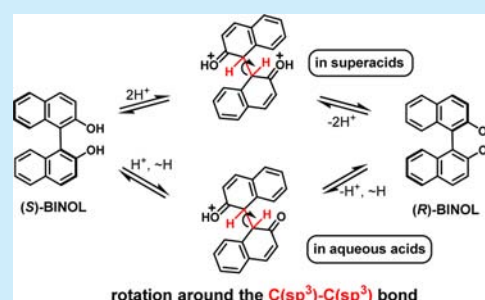


Protonation Behavior of 1,1'-Bi-2-naphthol and Insights into Its Acid-Catalyzed Atropisomerization

Alexander M. Genaev,[†] George E. Salnikov,^{†,‡} Andrey V. Shernyukov,[†] Zhongwei Zhu,[‡] and Konstantin Yu. Koltunov^{*,‡,§}[†]N. N. Vorozhtsov Novosibirsk Institute of Organic Chemistry, Pr. Akademika Lavrentieva 9, Novosibirsk 630090, Russia[‡]Novosibirsk State University, Pirogova 2, Novosibirsk 630090, Russia[§]Borisevsk Institute of Catalysis, Pr. Akademika Lavrentieva 5, Novosibirsk 630090, Russia

Supporting Information

ABSTRACT: The behavior of 1,1'-bi-2-naphthol (BINOL) in variety of (super)acid media has been studied by NMR. The results are combined with the theoretical (DFT) study of the role of mono- and diprotonated forms of BINOL in the acid-catalyzed atropisomerization of this compound. It is demonstrated that the process of enantiomeric configuration exchange proceeds mainly via internal rotation around the C1(sp³)–C1'(sp³) bond in intermediates such as C1-monoprotonated keto or C1,C1'-diprotonated forms of BINOL, depending on the acidity level.



BINOL (**1**) is currently one of the most versatile chiral reagents, which is the best known representative of axially chiral molecules. Numerous asymmetric reagents, catalysts, and materials have been prepared on the basis of atropisomers (*R*)-**1** and (*S*)-**1**.¹ Although practically resistant toward racemization under neutral conditions, **1** is known to racemize in both acidic and basic solutions.^{1,2} For instance, (*S*)-**1** is racemized 72% in 1.2 N HCl/1,4-dioxane at 100 °C for 24 h, and this sets rough limits of handling (*S*)-**1** or (*R*)-**1** without loss of optical purity in an acid medium.^{2a}

According to a widely accepted view, the acid-catalyzed atropisomerization of **1** proceeds via protonation on the C1 atom, which ensures the naphthyl ring rotation around the C(sp²)–C(sp³) bond (Scheme 1).^{1,2} By now, a variety of

Despite extensive theoretical studies, it is astonishing that the actual protonation behavior of **1** in acid solutions has not been investigated experimentally thus far (see, however, ref 3d, which concerns the failed attempt to generate a C-protonated form of **1** in neat HSO₃F). In contrast, the parent 2-naphthol is known to undergo exhaustive C1-protonation in superacid systems, such as HSO₃F–SO₂ClF or HSO₃F–SbF₅–SO₂ClF, to give ion **3** at low temperature (Figure 1).⁵ Moreover, 2-naphthol undergoes either C,C- or O,C-diprotonation in a stronger superacid, HF–SbF₅–SO₂ClF, to give dications **4** and **5** at –40 and –80 °C, respectively.^{5c}

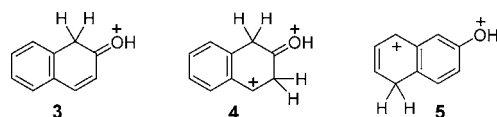
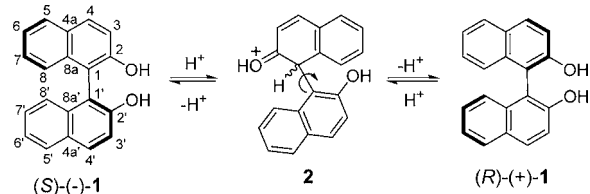


Figure 1. Long-lived mono- and dicationic species derived from 2-naphthol in superacids.⁵

Scheme 1. Generally Accepted Mechanism for the Acid-Catalyzed Atropisomerization of **1**

atropisomerization mechanisms for **1** under neutral, basic, and acidic conditions have been studied by DFT.³ In particular, it is calculated that among monoprotonated forms of **1** the most stable isomer is indeed that protonated on the C1 position (structure **2**, Scheme 1).⁴

Herein, we report NMR studies on the protonation behavior of **1** in various (super)acid media, representing the first experimental data in this regard. A comprehensive DFT study on the protonation of **1** as an aspect of its atropisomerization is also presented.

Taking into account that cationic species can sometimes be detected indirectly via H/D exchange with a deuterio acid, we have studied initially the deuteration of **1** under conditions typical for its atropisomerization. Thus, heating of (*S*)-**1** with 15% D₂SO₄–

Received: December 12, 2016

Published: January 17, 2017

D₂O/1,4-dioxane under reflux leads to notable racemization of the starting compound to give 11% of (*R*)-**1** after 15 h of reaction. According to ²H and ¹H NMR, the concurrent H/D exchange at carbon atoms occurs at positions (%) 8 (0.5) > 6 (0.4) > 3 (0.3), 4 (0.3), which conforms qualitatively to the values of *E*_{rel} of the corresponding monoprotonated forms of **1**.^{3d,4} However, the attained degree of deuteration (1.5% of total amount of protons) is too low for the involvement of the corresponding arenium ions in the racemization process. Obviously, the most feasible C1-deuterated form of **1**, which has to be formed in a greater extent, cannot be detected by this approach.

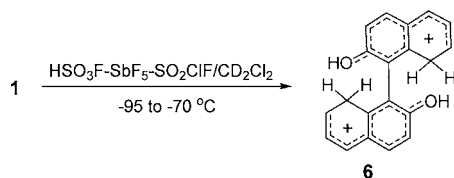
When dissolved in HSO₃F at room temperature, racemic **1** undergoes nonselective C-fluorosulfonation instead of forming carbocations. A number of signals of fluorine atoms belonging to different ArSO₂F moieties appear in the ¹⁹F NMR spectrum of the solution obtained, while the ¹H NMR spectrum looks similar to that reported earlier.^{3d}

Unexpectedly, dissolving **1** in neat CF₃SO₃H at room temperature leads to C1–C1' bond cleavage, giving ion **3** in an amount of 50% relative to the initial quantity of precursor. The missing part of the substance probably undergoes oligomerization, as indicated by broadened and unresolved NMR signals. Quenching of the solution with ice followed by extraction with diethyl ether gives only 2-naphthol along with traces of unidentified products (NMR and GC–MS data). The C–C bond-breaking mechanism is unclear now. A detailed study of this transformation is underway and will be reported elsewhere.

Furthermore, reaction of **1** with CF₃SO₃H–CF₃COOH (1:4 molar ratio) at room temperature does not produce long-lived protonated species. Instead, bis(trifluoroacetate) of **1** is mainly formed according to the ¹H, ¹⁹F, and ¹³C NMR spectral data. At that, no reaction at all is observed between **1** and neat CF₃COOH.

In contrast, protonation of **1** runs smoothly in HSO₃F–SbF₅ (1:1 molar ratio)–SO₂ClF–CD₂Cl₂ solution at –95 °C. According to NMR data (1D ¹H and ¹³C, 2D COSY, NOESY, HSQC, HMBC) (see the Supporting Information), **1** undergoes C8,C8'-diprotonation to form dication **6** (Scheme 2). Indicative

Scheme 2. Generation of Long-Lived Dication **6**



are the methylene AB spin system pattern at δ_{H} 4.35 and the corresponding aliphatic CH₂ signal at δ_{C} 40.4. It should be emphasized that the ²*J*_{HH} coupling constant in the methylene group (–30.7 Hz) shows a quite unusually high absolute value. The minus sign here is selected according to the CCSD/aug-cc-PVTZ calculations for benzenium ion (²*J*_{HH} = –33.4 Hz). NMR signals of protons bonded to oxygen atoms in **6** are not observed due to rapid proton exchange with the acid. Therefore, it cannot be excluded that the oxygen atoms also undergo protonation to form ultimately tetracationic species. We think, however, that a further protonation of **6** does not occur to any significant extent as the comparison of experimental and DFT/PBE/Λ22⁶ calculated ¹³C NMR chemical shifts reveals the root-mean-square deviation (RMSD) of 3.3, 9.3, and 14.4 ppm for **6**, O-protonated **6**, and O,O'-diprotonated **6**, respectively. The ¹H NMR spectrum of the dication **6** remains unchangeable with temperature increase up to

–70 °C. Further warming leads to irreversible changes in the spectrum, presumably due to reaction of **6** with CD₂Cl₂ in the presence of SbF₅.⁷

Dissolving **1** in a less acidic HSO₃F–SO₂ClF–CD₂Cl₂ system brought about the formation of the C1-protonated form **2**, along with mono- and diprotonated species **6**–**10** (Scheme 3, Figure 2).

Scheme 3. Ions Formed upon Protonation of **1** in HSO₃F–SO₂ClF–CD₂Cl₂

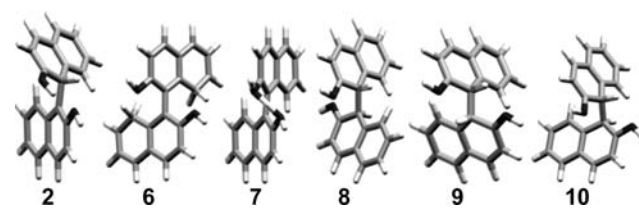
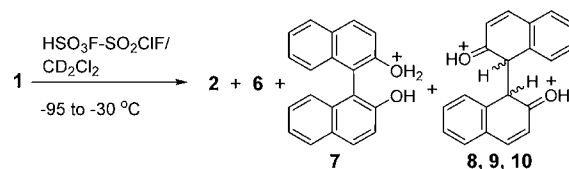


Figure 2. DFT/PBE/Λ1-optimized minimum energy geometries of ions **2** and **6**–**10**.

The same set of ions is also produced in CF₃SO₃H–CD₂Cl₂ at –40 °C, although in a slightly different ratio. Notably, the structures of all of these ions are determined unambiguously by NMR. Analysis shows that the ions concentration changes with time (Table 1), and it can be surmised that the O-

Table 1. Contents of Ions Formed from **1** in HSO₃F–SO₂ClF–CD₂Cl₂ as a Function of Time On-Stream at –91 °C (mol %)^a

time (h)	2	6	7	8	9	10	sum ^c
0.0 ^b	48.2	1.0	28.0	4.0	9.3	3.4	94.0
0.2	52.2	0.9	23.8	4.0	9.7	3.7	94.3
1.7	61.0	0.4	10.7	3.8	10.2	8.7	94.8
4.3	57.0	0.3	9.8	3.1	8.9	14.9	94.0
7.5	53.2	0.3	9.3	2.2	7.6	21.9	94.4
8.6	51.7	0.3	9.3	1.9	7.4	24.1	94.7

^aMeasured from ¹H NMR spectroscopic data using the HSO₃F signal as the internal standard for quantitative analysis. ^bAt –100 °C. ^cThe balance is unidentified species.

monoprotonated form **7** is generated initially. As the NMR signals of protons bonded to oxygen atoms in **7** are not observed directly, it may be assumed that this species is in fact bis(fluorosulfonate) of **1**. However, the C1 chemical shift in **7** (δ_{C} 113.9) is close to that in **1** (δ_{C} 110.8–114.3) rather than to those in bis(chlorosulfonate), bis(triflate), and bis(trifluoroacetate) of **1** (δ_{C} 123.2–123.6, see the SI and ref 8). The presence of protons bonded to oxygen atoms in **7** is revealed by NOE cross peaks between the signals of H3,3' and the region covering mutually overlapping and exchanging resonances of OH, OH₂⁺, and the acid protons. The proposed structure of cation **7** is also preferable to O,O'-diprotonated form of **1**, as it has a lower RMSD of experimental and DFT/PBE/Λ22 calculated ¹³C NMR chemical shifts (3.5 ppm vs 13.3 ppm, respectively). Analogously, NMR signals of protons bonded to oxygen atoms in monocation **2** are observed only for the C1-protonated naphthalene ring, but the

probable formation of the C1,O'-diprotonated **1** instead of **2** can be excluded by its higher RMSD (7.4 vs 3.2 ppm, respectively). Likewise, cation **2** cannot be a fluorosulfonate as NOE cross peaks between the signals of H1, H3', and H8 and the acid signal region indicate that the substituent at the C2' position is OH and not OSO₂F. The proposed spatial structure of **2** is also in agreement with the NMR data. Thus, the H8' signal is strongly shielded (δ 6.23 ppm), as expected for the most stable conformation of **2** predicted by DFT calculations (Figure 2).

As seen from the time course of the ion contents (Table 1), cation **7** is transformed into monocation **2** and, more slowly, into several C1,C1'-diprotonated species. Although DFT/PBE/Å1 conformational analysis yields as many as 17 possible diastereomers and conformers of C1,C1'-diprotonated **1**, only three of them, namely **8–10**, are actually observed by NMR. The same structures are the most stable according to DFT calculations, in the order of **10** > **9** > **8**. Indeed, the most stable conformer **10** is the only one whose content steadily increases in time (Table 1). The ROESY spectrum of **10** shows strong cross peaks corresponding to NOE between protons in pairs H8–H1' and H1–OH', which is in agreement with the spatial proximity of these protons in the calculated geometry of **10**. The chemical shifts of H8 and H8' are highly indicative as well, due to either shielding or deshielding effects by the opposite naphthalene moiety. Thus, in dication **10** the H8 and H8' protons are nonequivalent and resonate at δ 8.22 and 6.52, whereas in **8** and **9** these protons are equivalent and resonate at δ 8.16 and 6.62, respectively. In a stereochemical aspect, dications **8** and **9** are stable conformational isomers of each other, and both are diastereomers of **10**.

Also, it can be noticed in Table 1 that the content of dication **6** is directly proportional to that of monocation **7** and is about 30 times lower. Apparently, these species are in equilibrium. We believe that in the more strongly acidic HSO₃F–SbF₅–SO₂ClF–CD₂Cl₂ system the initially formed **7** is protonated further to give O,O'-diprotonated **1**, which immediately undergoes intramolecular rearrangement into **6** (DFT barrier is 0.4 kcal mol^{−1}, i.e., actually below the accuracy of the method, see the SI). Dication **6**, although thermodynamically less stable than **8–10**, has a high kinetic stability. Conversion of **6** into **8–10** would require its preliminary deprotonation, which is hardly possible in a strongly acidic medium.

According to DFT calculations, the dihedral angle H1–C1–C1'–H1' in **8–10** is close to 90°. As shown in Figure 3, the 180° internal rotation around the C1–C1' bond changes the enantiomeric configuration of these dications, converting (R)-**10** into (S)-**10**, and (R)-**9** into (S)-**8** (and vice versa); the rotation is more facile when it proceeds via intermediates having H1 and H1' atoms in the anti position. Notably, these rotation processes in dications **8–10** are confirmed unambiguously by the corresponding exchange cross peaks in ROESY and NOESY spectra (at −91 °C).

With an increase in temperature, the H1 and H1' signals of **8–10** undergo significant line broadening and eventually merge into one central peak (Figure 4). Using the Eyring equation, we have calculated the values of $\Delta H^\ddagger = 10.7 \pm 0.5$ kcal mol^{−1}, $\Delta S^\ddagger = -0.7 \pm 2.2$ cal mol^{−1} K^{−1}, and $\Delta G^\ddagger = 10.8$ kcal mol^{−1} (at −91 °C) for the conformational exchange in **10**. From NOESY data, we have also estimated the value of $\Delta G^\ddagger \approx 10.6$ kcal mol^{−1} for the conformational exchange between **9** and **8** at −91 °C (equilibrium constant **9/8** \approx 3, rate constant $k_{9 \rightarrow 8} \approx 0.7$ s^{−1}). The experimental values of ΔG^\ddagger for the conformational exchange in **8–10** are practically coincident with the rotational barriers calculated by

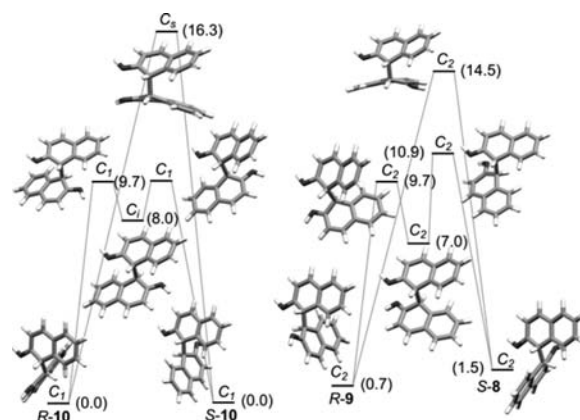


Figure 3. Energy diagrams and optimized geometries of the corresponding transition states and intermediates (DFT/PBE/Å1) for the internal rotation around the C1–C1' bond in dications **8–10**. Relative free energy values (ΔG at −91 °C) are given in kcal mol^{−1}. Prefixes R and S denote the stereochemical relationship between the naphthalene skeletons.

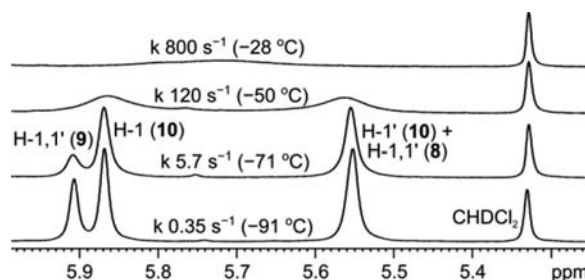


Figure 4. Temperature dependence of DNMR spectra (600 MHz, H1 protons region) of **1** dissolved in HSO₃F–SO₂ClF–CD₂Cl₂. The rate constant values correspond to the conformational exchange in **10**.

DFT (Figure 3). Hence, the observed dynamics process relates entirely to the enantiomeric configuration change in dications **8–10**, and these dications can be regarded as intermediates in atropisomerization of **1** under superacid conditions.⁹

However, their intermediacy under weak acid conditions is unlikely. Indeed, according to earlier estimations, atropisomerization of **1** via C1,C1'-diprotonated form is only reachable provided that the ratio of neutral **1** to C1,C1'-diprotonated **1** in 1.2 N HCl does not exceed 10¹¹.^{3d} Considering, for example, dication **10** as a dibasic acid, we can derive the following equations

$$\lg 10/2 = pK_{10} - H_0 \quad (1)$$

$$\lg 2/1 = pK_2 - H_0 \quad (2)$$

where K_{10} and K_2 are the acid dissociation constants of **10**. Consequently

$$\lg 10/1 = \lg 10/2 + \lg 2/1 = pK_{10} + pK_2 - 2H_0 \quad (3)$$

According to our data, concentrations of **10** and **2** in HSO₃F–SO₂ClF–CD₂Cl₂ are comparable; therefore, the value of pK_{10} should be of the same order as $H_0 = -1.5$ for HSO₃F. The value of pK_2 should have roughly the same magnitude as $pK_a = -8$ for monoprotonated **1** measured by NMR titration (see the SI). Substituting these approximations into eq 3 allows estimation of the **1/10** ratio at different acidity levels. For example, in 1.2 N HCl ($H_0 = -0.3$) the value of **1/10** should be about 10²², which is much higher than the limit of **1/10** = 10¹¹. The same is generally true of dications **9** and **8**.

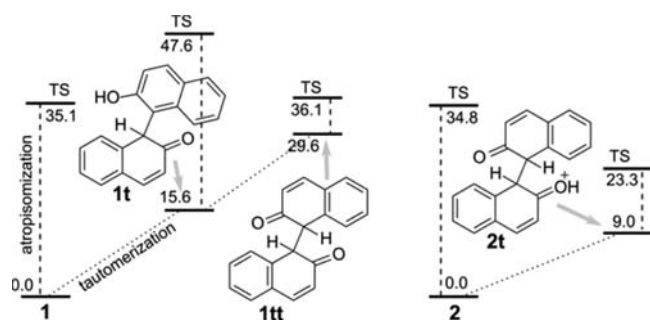


Figure 5. Relative energies and barriers of internal rotation around the C1–C1' bond for **1**, **2**, and their tautomeric keto forms (DFT/PBE/Δ1, kcal mol^{−1}).

Considering participation of monocation **2** as potential intermediate in atropisomerization of **1**, it should be noted that rotation around the C1–C1' bond in **2** is almost as difficult as in the neutral precursor **1** (Figure 5). However, the rotation can proceed much easier through the tautomeric form **2t**, in spite of its relative instability. The preliminary conversion **2** → **2t** decreases the total rotational barrier in **2** to 23.3 kcal mol^{−1}, which is surmountable already at room temperature (as follows from Eyring's equation). Notably, generation of tautomer **2t** does not require the intermediacy of dications **8–10** as it can be formed from **2** via a proton transfer mechanism analogous to the acid-catalyzed tautomerization mechanism of 2-naphthol.¹⁰ Based on the experimental atropisomerization barrier of **1** in 1.2 N HCl/1,4-dioxane ($\Delta G^\ddagger = 30.4$ kcal mol^{−1} at 362 K)^{3d} and taking into account the concentration of ions **2** in this medium ($2/1 = 10^{-7.7}$) found by eq 2, the atropisomerization barrier for **2** is estimated to be 17.6 kcal mol^{−1}. This is somewhat less than the calculated value of 23.3 kcal mol^{−1}. The latter, however, comes to an agreement with the expected value after application of the solvent and dispersion corrections (SI).

Even easier is the rotation around the C1–C1' bond in a neutral diketeto form **1tt**, but due to the higher relative energy of **1tt** itself, the total barrier of 36.1 kcal mol^{−1} seems prohibitive. Rotation around the C1–C1' bond in the neutral keto form **1t** appears to be the most unfavorable.

In summary, on the basis of the protonation behavior of **1** revealed by NMR and DFT calculations, it is demonstrated that atropisomerization of **1** proceeds mainly via rotation around the C(sp³)–C(sp³) bond in intermediates such as the C1,C1'-diprotonated forms **8–10**, C1-monoprotonated keto form **2t**, and diketeto form **1tt**. However, their relative contribution depends on the acidity level of the reaction medium. Dications **8–10** can actually participate in the reaction only in superacids ($H_0 < -12$), while monocation **2t** is the most feasible intermediate under moderate acidity conditions.

■ ASSOCIATED CONTENT

Supporting Information

The Supporting Information is available free of charge on the ACS Publications website at DOI: 10.1021/acs.orglett.6b03696.

Experimental procedures, NMR spectra, and computational data (PDF)

■ AUTHOR INFORMATION

Corresponding Author

*E-mail: koltunov@catalysis.ru.

ORCID

Konstantin Yu. Koltunov: 0000-0002-9466-1592

Notes

The authors declare no competing financial interest.

■ ACKNOWLEDGMENTS

G.E.S. and A.M.G. gratefully acknowledge the support of the RFBR under Grant No. 16-03-00357. We also acknowledge Cluster of the Information Computation Center, Novosibirsk State University (<http://www.nusc.ru/>) for computing resources and the Multi-Access Chemical Service Center SB RAS for spectral measurements and thank Prof. K. P. Bryliakov (Boreskov Institute of Catalysis) for conducting HPLC–UV enantiomeric ratio analysis.

■ REFERENCES

- (1) (a) Brunel, J. M. *Chem. Rev.* **2005**, *105*, 857–897. (b) Chen, Y.; Yekta, S.; Yudin, A. K. *Chem. Rev.* **2003**, *103*, 3155–3212. (c) Kocovsky, P.; Vyskocil, S.; Smrcina, M. *Chem. Rev.* **2003**, *103*, 3213–3246. (d) Pu, L. In *1,1'-Binaphthyl-Based Chiral Materials: Our Journey*; Imperial College Press: London, 2010. (e) Schenker, S.; Zamfir, A.; Freund, M. S.; Tsogoeva, B. *Eur. J. Org. Chem.* **2011**, *2011*, 2209–2222. (f) Parmar, D.; Sugiono, E.; Raja, S.; Rueping, M. *Chem. Rev.* **2014**, *114*, 9047–9153.
- (2) (a) Kyba, E. P.; Gokel, G. W.; de Jong, F.; Koga, K.; Sousa, L. R.; Siegel, M. G.; Kaplan, L.; Sogah, G. D. Y.; Cram, D. J. *J. Org. Chem.* **1977**, *42*, 4173–4184. (b) Yudin, A. K.; Martyn, L. P. J.; Pandiaraju, S.; Zheng, J.; Lough, A. *Org. Lett.* **2000**, *2*, 41–44.
- (3) (a) Sahnoun, R.; Koseki, S.; Fujimura, Y. *J. Mol. Struct.* **2005**, *735*, 736–736, 315–324. (b) Da, L.-G.; Lu, T.-T.; Xiang, M.; He, T.-J.; Chen, D.-M. *Chin. J. Chem. Phys.* **2008**, *21*, 367–375. (c) Meca, L.; Reha, D.; Havlas, Z. *J. Org. Chem.* **2003**, *68*, 5677–5680. (d) Alkorta, I.; Cancedda, C.; Cocinero, E. J.; Dávalos, J. Z.; Écija, P.; Elguero, J.; González, J.; Lesarri, A.; Ramos, R.; Reviriego, F.; Roussel, C.; Uriarte, I.; Vanthuyne, N. *Chem. - Eur. J.* **2014**, *20*, 14816–14825.
- (4) Our results on the computational study of monoprotonated forms of **1** are close to those reported previously (ref 3d), although we succeeded in finding several conformers with lower energy. The updated series of monoprotonated **1** is as follows (E_{rel} , kcal mol^{−1}): C1 (0.0) > C8 (2.0) > C6 (4.9) > C3 (7.5) > C4 (7.8) > C5 (10.0) > O (11.4) > C7 (11.8) > C2 (23.2).
- (5) (a) Olah, G. A.; Mateescu, G. P.; Mo, Y. K. *J. Am. Chem. Soc.* **1973**, *95*, 1865–1874. (b) Repinskaya, I. B.; Shakirov, M. M.; Koltunov, K. Yu.; Koptiyug, V. A. *J. Org. Chem. USSR* **1992**, *28*, 778–784. (c) Repinskaya, I. B.; Koltunov, K. Yu.; Shakirov, M. M.; Koptiyug, V. A. *J. Org. Chem. USSR* **1992**, *28*, 785–795.
- (6) (a) Perdew, J. P.; Burke, K.; Ernzerhof, M. *Phys. Rev. Lett.* **1996**, *77*, 3865–3868. (b) Laikov, D. N. *Chem. Phys. Lett.* **1997**, *281*, 151–156. (c) Laikov, D. N.; Ustynyuk, Y. A. *Russ. Chem. Bull.* **2005**, *54*, 820–826. (d) Laikov, D. N. *Chem. Phys. Lett.* **2005**, *416*, 116–120.
- (7) Salnikov, G. E.; Genaev, A. M.; Bushmelev, V. A.; Nefedov, A. A.; Shubin, V. G. *RSC Adv.* **2014**, *4*, 52831–52835.
- (8) (a) Woeste, T. H.; Oestreich, M. *Chem. - Eur. J.* **2011**, *17*, 11914–11918. (b) Berkessel, A.; Christ, P.; Leconte, N.; Neudörfl, J.-M.; Schäfer, M. *Eur. J. Org. Chem.* **2010**, *2010*, 5165–5170.
- (9) In contrast to intermediates **8–10**, cation **2** and dication **6** are not considered as significant contributors to atropisomerization of **1**. Indeed, cation **2** does not show DNMR line broadening and NOESY/EXSY cross peaks, and the calculated barriers to rotation around the C1–C1' bond in **2** (34.8 kcal mol^{−1}) and **6** (38.3 kcal mol^{−1}) are too high.
- (10) (a) Raczynska, E. D.; Kosinska, W.; Osmialowski, B.; Gawinecki, R. *Chem. Rev.* **2005**, *105*, 3561–3612. (b) Jacobsson, M.; Oxgaard, J.; Abrahamsson, C.-O.; Norrby, P.-O.; Goddard, W. A., III; Ellervik, U. *Chem. - Eur. J.* **2008**, *14*, 3954–3960.